VILNIAUS UNIVERSITETAS

FIZINIŲ IR TECHNOLOGIJOS MOKSLŲ CENTRAS

PAULIUS STANISLOVAITIS

ŠVIESOS SŪKURIŲ FORMAVIMAS IR JŲ TIESINĖS BEI NETIESINĖS TRANSFORMACIJOS

Daktaro disertacijos santrauka

Fiziniai mokslai, fizika (02 P)

Vilnius, 2017

Disertacija rengta 2013-2017 metais Vilniaus universiteto fizikos fakulteto kvantinės elektronikos katedros lazerinių tyrimų centre.

Mokslinis vadovas – prof. habil. dr. Valerijus Smilgevičius (Vilniaus universitetas, fiziniai mokslai, fizika – 02 P).

Disertacija ginama viešame Gynimo tarybos posėdyje :

Pirmininkas :

prof. habil. dr. Arūnas Krotkus (Fizinių ir technologijos mokslų centras, fiziniai mokslai, fizika – 02P).

Nariai :

dr. Gintaras Valiulis (Vilniaus universitetas, fiziniai mokslai, fizika – 02 P),

dr. Valdas Pašiškevičius (Švedijos karalškasis technologijos institutas, fiziniai mokslai, fizika – 02 P),

dr. Kęstas Regelskis (Fizinių ir technologijos mokslų centras, fiziniai mokslai, fizika – 02P)

dr. Sergėjus Orlovas (Fizinių ir technologijos mokslų centras, fiziniai mokslai, fizika – 02P)

Disertacija bus ginama viešame tarybos posėdyje 2017 m. rugsėjo mėn. 28 d. 15 val. Fizikos fakulteto 214 auditorijoje.

Adresas : Saulėtekio al. 9, LT-10222, Vilnius, Lietuva

Disertacijos santrauka išsiuntinėta 2017 m. rugpjūčio mėn. 28 d.

Disertaciją galima peržiūrėti Vilniaus universiteto, Fizinių ir technologijos mokslo centro bibliotekose ir VU interneto svetainėje adresu: *www.vu.lt/lt/naujienos/ivykiu-kalendorius*

VILNIUS UNIVERSITY

CENTER FOR PHYSICAL AND TECHNOLOGICAL SCIENCES

PAULIUS STANISLOVAITIS

GENERATION OF OPTICAL VORTICES AND THEIR LINEAR AND NONLINEAR TRANSFORMATIONS

Doctoral Dissertation Summary

Physical Sciences, physics (02 P)

Vilnius, 2017

The research described in this thesis has been perfomed in 2013-2017 in Vilnius university, faculty of physics, department of quantum electronics, laser research center.

Scientific supervisor - prof. habil. dr. Valerijus Smilgevičius (Vilnius University, Physical sciences, physics - 02 P)

The dissertation will be defended at the public session of the council :

Chairman :

prof. habil. dr. Arūnas Krotkus (Center for Physical Sciences and Technology, physical sciences, physics - 02P)

Members :

dr. Gintaras Valiulis (Vilnius university, physical sciences, physics - 02P)

dr. Valdas Pašiškevičius (Royal Institute of Tecnology, Sweden, physical sciences, physics - 02P)

dr. Kęstas Regelskis (Center for Physical Sciences and Technology, physical sciences, physics - 02P)

dr. Sergėjus Orlovas (Center for Physical Sciences and Technology, physical sciences, physics - 02P)

The dissertation will be defended in a public session of the council at the faculty of physics, room 214, on the 28th of September 2017 at 3 PM.

Address : Saulėtekio Ave. 9, LT-10222, Vilnius, Lithuania.

The dissertation summary has been distributed on the 28th ofAugust, 2017.

The dissertation is available in VU libraries and online at *www.vu.lt/lt/naujienos/ivykiu-kalendorius*

Contents

1 Introduction, goals of the work and thesis statements **1**

2 Literature overview **5**
2.1 Dislocations in wavefronts 5
2.2 Nonlinear transformations of optical vortices in a quadratic-nonlinearity medium 7
2.3 Generation of the optical vortex beams 7
2.3.1 Generation of optical vortex by a radial polarization converter 9

3 Generation of unit- and half-charged optical vortex by a radial polarization converter **10**
3.1 The Jones matrix of a radial polarization converter 10
3.2 The influence of the wavelength mismatch on the beams, formed by the radial polarization converter 11
3.3 Creation of optical vortices by a radial polarization converter 11
3.4 The Experiment 12
3.5 Conclusions 13

4 Formation of doubly charged optical vortices by radial polarization converter by using a double-pass technique **14**
4.1 Effect of radial polarization converter on optical vortices 14
4.2 The principle of the double-pass technique 15
4.3 The Experiment 17
4.4 Conclusions 18

5 Control of optical vortex positions by interference **19**
5.1 Collinear interference of the Laguerre-Gaussian beams 19
5.2 The Experiment 21
5.3 Conclusions 22

6 Conservation of topological charge in a second harmonic generation process for fractional-charge optical vortices **23**
6.1 The dilemma of topological charge conservation of fractional-charge optical vortices 23
6.2 Topological charge conservation in the second harmonic generation process 24
6.3 The Experiment 25
6.4 Conclusions 26

7 Generation of beams with polarization singularities using the optical parametric amplification of optical vortices **27**
7.1 Generation of beams with polarization singularities by superposition of Laguerre-Gaussian modes 27
7.2 The general idea of the method 28
7.3 Experimental 30
7.4 Conclusions 30

8 The main results and conclusions **31**

1. Introduction, goals of the work and thesis statements

For the first time dislocations in wavefronts were described by Nye and Berry in 1974 [1]. These dislocations are common to all types of waves, whether it is sound or electromagnetic waves. There are three types of such dislocations : the screw dislocation (I), the edge dislocation (II) and the mixed screw-edge dislocation (III). The screw dislocations in light waves are also called "Optical Vortices" [2]. The light intensity at these dislocations is zero wavefronts helical. They are stable and do not disappear during propagation. Optical vortices are a widely researched topic today. Due to their unique properties they have found their way into applications such as optical trapping of particles[3], STED microscopy [4] and other...

Other types of wavefront dislocations exist as well. For example, edge dislocations manifest as dark lines in the intensity pattern of a beam, which do not disappear as the beam propagates. Edge dislocations can be either infinite (like in Hermite-Gaussian modes) or closed (like in Laguerre-Gaussian modes with radial index higher than 0).

In addition, there is a third type of dislocations - the mixed screw-edge dislocations, sometimes called the "fractional topological charge optical vortices". These dislocations are unstable and upon propagation transform into optical vortices with the nearest topological charge [5, 6].

In this work most of the attention is dedicated to the screw dislocations, that is, the optical vortices. In addition, some parts of this work are dedicated to the mixed screw-edge dislocations as well as polarization singularities.

The goals of this work

1. To analyze theoretically and show experimentally a computer-controlled motion of optical vortex dislocations by means of interference.

2. To theoretically investigate a possibility to generate half-charged optical vortices using a radial polarization converter and to test this idea experimetally.

3. To theoretically investigate a possibility to generate doubly-charged vortices using a radial polarization converter and to test this method experimentally.

4. To investigate theoretically and experimentally whether or not the topological charge conservation holds true for mixed screw-edge dislocations in the second harmonic generation process.

5. To analyze and demonstrate experimentally a new method which allows to create beams with polarization singularities using the optical parametric amplification of optical vortices.

The novelty of the results

1. A computer-controlled optical vortex motion based on interference was implemented experimentally.

2. A wavelength mismatch effects on the operation of the radial polarization element was analyzed and a new method was proposed to form a half-charged optical vortices.

3. A new method was proposed to create a double-charged vortices using a radial polarization converter.

4. Some of the properties of the half-charged optical vortices have been investigated and the validity of the topological charge conservation law was confirmed in the second harmonic generation process.

5. A new method to create beams with polarization singularities has been proposed, analyzed and experimentally demonstrated.

Thesis Statements

1. It is possible to position optical vortices precisely in light beams using a collinear interference with a Gaussian beam and manipulating the beam's phase and intensity. The positions of the vortex cores depend on the intensity ratio and the phase difference between the two interfering beams.

2. By using a radial polarization converter, it is possible to generate half-charged optical vortices by converting light of double wavelength compared to the converter's nominal wavelength.

3. By using a double pass-technique, not only a singly, but also a doubly-charged optical vortex can be generated using only a single radial polarization converter. While the converter can be manufactured for optical vortices of any topological charge, this method can double that topological charge.

4. Despite the inherent instability of a half-charged vortex and its transformation into a unit-charged vortex, the topological charge conservation law holds true for half-charged optical vortices in the second harmonic generation process and a unit-charged vortex is observed in the second harmonic beam.

5. By optical parametric amplification of optical vortices in a nonlinear crystal with type-II phase matching and subsequent conversion by a $\lambda/2$ waveplate, beams with polarization singularities can be obtained, including radially and azimuthally polarized beams.

Author's publications

Publications in scientific juornals

[P1] P. Stanislovaitis, V. Smilgevičius. Control of optical vortex dislocations using optical methods. Lietuvos Fizikos Žurnalas 52(4), p. 295-300 (2012)

[P2] P. Stanislovaitis, V. Smilgevičius. Peciliarities of second harmonic generation by paraxial beams with radial/azimuthal polarization in type II nonlinear crystal. Lietuvos fizikos žurnalas 54(3) (2014)

[P3] A. Matijošius, P. Stanislovaitis, T. Gertus, V. Smilgevičius. Formation of optical vortices with topological charge $|l| = 1$ and $|l| = 1/2$ by use of the S-waveplate, Optics Communications 324, p. 1-9 (2014)

[P4] A. Matijošius, P. Stanislovaitis, T. Gertus, V. Smilgevičius. Formation of second order optical vortices with a radial polarization converter using the double-pass technique, Optics Communications 349, p. 24-30, 2015

[P5] P. Stanislovaitis, A. Matijošius, M. Ivanov, V. Smilgevičius. Topological charge transformation of beams with embedded fractional phase step in the process of second harmonic generation, accepted to Journal of Optics (2017)

Participation in scientific conferences

[K1] P. Stanislovaitis, V. Smilgevičius. Pecularities of second harmonic generation by paraxial beams with radial/azimuthal polarization in type II nonlinear crystal, 20-tas Lietuvos-Baltarusijos seminaras „Lazeriai ir optinis netiesiškumas“, Vilnius,

2014

[K2] P. Stanislovaitis, A. Matijošius, T. Gertus, V. Smilgevičius. Formation of optical vortices with topological charge $|l| = 2$ using the radial polarization converter, Open readings 2014, Vilnius

[K3] P. Stanislovaitis, A. Matijošius, V.Smilgevičius, M. Ivanov. Topological charge conservation of optical vortices with topological charge $l = 1/2$ in second harmonic generation process. ICONO/LAT 2016, Minskas

[K4] P. Stanislovaitis, V. Smilgevičius. Control of optical vortex dislocations using optical methods, 39-oji Lietuvos Nacionalinė Fizikos Konferencija, 2011, Vilnius

The author's presonal contribution

The author suggested some of the thesis objectives and offered their solution, also carried out theoretical analysis, numerical modeling and participated in writing of the publications as well as presented the experimental results in scientific conferences.

2. Literature overview

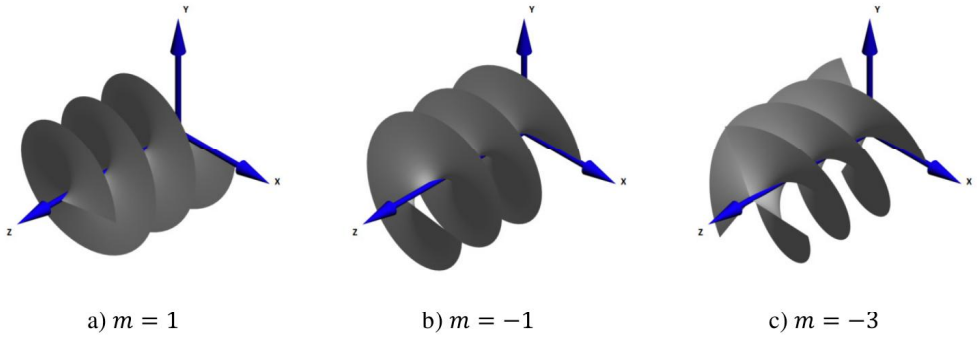

Figure 2.1: Examples of helical wavefronts with different topological charges : 1 (a), -1 (b) ir -3 (c).

Dislocations in wavefronts

In optical waves, the screw dislocations are called "Optical vortices" [2]. Around such a dislocation, the wavefront is helical in form. The multiplicity and winding direction of the wavefront is described by the parameter called the "topological charge". In fig. 2.1, some examples of helical wavefronts are given width different topological charges.

The optical vortices are stable upon propagation and the dark spot does not disappear, as it would otherwise, if the beam did not have the helical wavefront. However, dislocations with higher than unit topological charge are unstable and if there is a coherent background, they decay into unit-charged dislocations [7, 8]. Examples of optical vortices are the Laguerre-Gaussian modes. One useful property of optical vortices is that they carry the orbital angular momentum [9, 10, 11]. This property is exploited in optical tweezers and spanners to rotate microscopic objects [12].

Another interesting property of optical vortices that has been investigated is the self-reconstruction of the beam. When a part of the vortex beam is blocked, it has been shown that during the propagation they reconstruct [13, 14, 15, 16, 17]. Optical

vortices have been shown to reconstruct even if their central dark core was blocked [16].

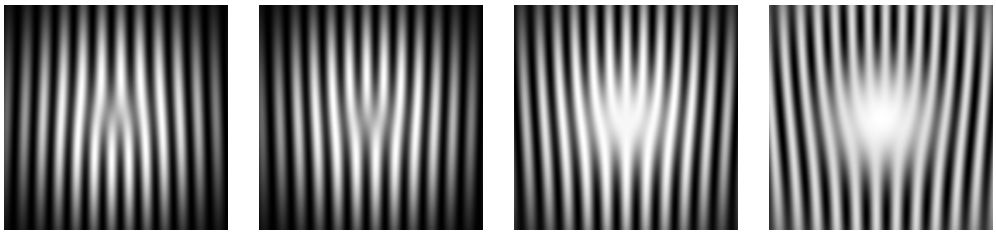

m = -1 m = 1 m = 2 m = 3

Figure 2.2: The inerference of optical vortices with a Gaussian beam. The topological charge is denoted by m.

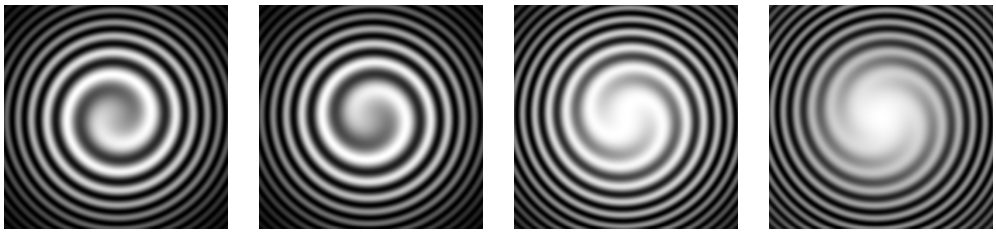

m = -1 m = 1 m = 2 m = 3

Figure 2.3: A collinear interference between an optical vortex and a Gaussian beam when the curvature radii of the beams are different.

Optical vortices also have their characteristic interference patterns. When an optical vortex interferes with a simple Gaussian beam, one of the fringes is forked at the position of dislocations. The quantity of new fringes that appear indicates the topological charge of the vortex and the fork's direction - its sign (fig. 2.2). Also, optical vortices are sometimes analyzed using a Michelson interferometer. In this case, the optical vortex interferes with itself. The center of optical vortex interferes with the edge of it, thus also producing the forked interference pattern.

Apart from screw dislocations there are also edge dislocations and mixed screw-edge dislocations. The edge dislocations are lines in the intensity pattern where there is a sudden phase shift of π. These dislocations can be either infinite (like in Hermite-Gaussian modes or closed (like, for example, in the Bessel beams [18]).

Also Nye and Berry suggests that there is a third type of dislocations - the mixed screw-edge dislocations. They are also referred to as the "fractional-charge optical vortices". It was shown that these dislocations are unstable and transform into integer charged dislocations of the nearest topological charge [6, 19, 5].

In this work we mostly dedicate our attention to optical vortices and mixed screw-

edge dislocations.

Nonlinear transformations of optical vortices in a quadratic-nonlinearity medium

There are numerous publications dedicated to nonlinear optics of singular beams [20, 21, 22, 23, 24, 25, 26, 27, 28]. Soskin and Vastnetsov in their work [20] suggested the following generalizations :

1) All known nonlinear phenomena can be also observed for beams with helical wavefront. Often they show some peculiarities that are connected with helical wavefront, integer topological charge and orbital angular momentum.

2) In the collinear sum and frequency difference generation, the topological charge conservation law holds true.

3) A low intensity CW laser radiation can create optical vortex solitons in a focusing as well as defocusing medium.

4) Arrays of optical vortices wit a zero net topological charge can appear due to astigmatic Gaussian lens appearing in anisotropic media.

There are a lot of works dedicated to the second harmonic generation [21, 22], sum [26, 27] and difference [28] frequency generation, parametric fluorescence [29, 30, 31] as well as optical vortex transformation in a cubic nonlinearity media [32, 33, 34, 35, 36, 37].

One of the ideas, suggested by Soskin - the law of topological charge conservation. In a collinear three wave interaction, where the frequencies of waves are such that $\omega_3 > \omega_1, \omega_2$, a relation between the topological charges of these waves holds true :

$$l_3 = l_1 + l_2 \ . \tag{2.1}$$

The only case when this is not apparent is the parametric fluorescence when the signal and idler waves are created from the quantum noise. The topological charge conservation seems to hold true even in seeded second harmonic generation [24].

Generation of the optical vortex beams

There are numerous methods of generating optical vortex beams, such as the printed holograms [38, 39, 40, 41, 42], spiral phase plates and phase holograms [43, 44, 45, 46, 47], spatial light modulators [48, 49, 50, 51, 52, 53], cylindrical-lens mode

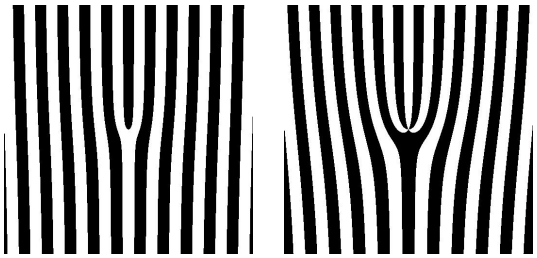

(a) (b)

Figure 2.4: Binary optical vortex holograms that are simpler to print by printer l=1 (a) and l=3 (b).

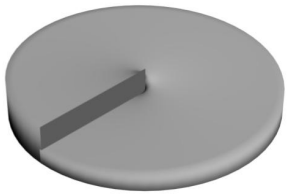

Figure 2.5: A spiral phase plate for generation of optical vortices.

converters [54, 55, 56, 57, 58, 59], the S-waveplate (the radial polarization converter) [60, 61] , inside the laser resonator [63, 64, 65, 66, 67, 68, 69], microspheres [70] and a deformable mirror [71, 72, 73].

Probalby the first and the easiest method is generation of otpical vortices by printed holograms [38, 39, 40, 41, 42]. A forked diffraction granting is printed with a printer on a transparent film (fig. 2.4). This an easy method to create optical vortices, only not very efficient. Most of the beam's energy goes into a non-useful central maximum as well as into other maxima. In addition, the holograms have a low optical damage threshold and tend to degrade over time. While this method is probably the easiest of all, it is very inefficient and does not allow the generation of intense optical vortex beams.

Optical vortices can be created by using phase holograms as well as spiral phase plates [43, 44, 45, 46, 47]. The spiral phase plate is an optical element with its thickness varying in the angular direction. It has a ramp, the height of which depends on the intended topological charge of the vortex. It is shown in fig. 2.5.

Also phase holograms can also be manufactured to deflect the optical vortex by an angle. The advantage of such holograms is that they don't absorb much light and can withstand higher intensities than simple printed holograms. Therefore the efficiency is much higher and it is possible to create more intensive optical vortices, suitable for nonlinear optics experiments. However, such plates are difficult to manufacture.

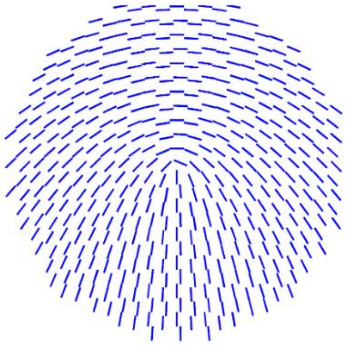

Figure 2.6: Orientations of the principal axes in the radial polarization converter [60].

Generation of optical vortex by a radial polarization converter

One of the methods used in this work to create optical vortices is the radial polarization converter (S-waveplate) [60, 61]. The radial polarization converter is essentially a spatially-variant $\lambda/2$ waveplate with the direction of the optical axis depending on the azimuthal angle (fig. 2.6). While it is meant for generation of a radially or azimuthally polarized beam, for a circularly polarized light it acts as a phase plate, forming a unit-charged optical vortex.

3. Generation of unit- and half-charged optical vortex by a radial polarization converter

In this chapter we review a method to generate a unit-charged optical vortex by a radial-polarization converter (also called the S-waveplate) [61] and discuss a method to create a half-charged optical vortex. The results of this work have been published in the article [P3].

The Jones matrix of a radial polarization converter

In principle, the radial polarization converter [61, 60] is a $\lambda/2$ waveplate, with its principal axis depending on the azimuthal angle. The Jones matrix of a radial polarization converter is :

$$\widehat{A} = \begin{bmatrix} \cos\phi & \sin\phi \\ \sin\phi & -\cos\phi \end{bmatrix} . \tag{3.1}$$

Therefore the radial polarization converter is described by a Jones matrix $\widehat{A}$ in eq. (3.1). The radial polarization converter transforms linearly polarized light into radially/azimuthally polarized light or a superposition of both, depending on the direction of the polarization of the incoming light. If the incoming light has a circular polarization, then the converter works as a phase plate and converts it to an optical vortex [61].

If the polarization of incoming light has components v_x and v_y, using the converter's Jones matrix, the output polarization vector can be written in polar coordinates :

$$\vec{w}_{pol} = \begin{bmatrix} v_x \\ -v_y \end{bmatrix} . \tag{3.2}$$

Therefore, from eq. (3.2) it can be seen that the radial polarization converter transforms the beam's x component into the radial polarization and the y component to the azimuth polarization.

The influence of the wavelength mismatch on the beams, formed by the radial polarization converter

Let us assume that a beam is passing through the radial polarization converter which has a different wavelength than the converter was designed for. In this case the converter no longer works as a $\lambda/2$ waveplate. It will create a phase difference θ between the two orthogonal polarization components. Then, the radial polarization element's matrix can be shown to be:

$$\widehat{B} = \begin{bmatrix} \cos\phi & \sin\phi \\ \sin\phi & -\cos\phi \end{bmatrix} + (\mathrm{e}^{\mathrm{i}\theta} + 1) \begin{bmatrix} \sin^2\frac{\phi}{2} & \cos\frac{\phi}{2}\sin\frac{\phi}{2} \\ \cos\frac{\phi}{2}\sin\frac{\phi}{2} & \cos^2\frac{\phi}{2} \end{bmatrix} . \tag{3.3}$$

We can see that the radial polarization matrix consists of two summands (eq. 3.3): the radial polarization converter's matrix (as in eq. 3.1) and the additional component (the background part). By inserting $\theta = \pi$ we can see, that the background part actually vanishes.

Creation of optical vortices by a radial polarization converter

As discussed previously, the radial polarization converter can be used to create a unit-charged optical vortex from a circularly polarized light. Another interesting case is when the converter is used to convert the light with double its nominal wavelength. Then, in eq. 3.3, the phase shift will be $\theta = \pi/2$. If the input polarization vector is

$$\vec{v} = \begin{bmatrix} 1 \\ \mathrm{i} \end{bmatrix} , \tag{3.4}$$

multiplying it by the matrix $\widehat{B}$ in eq. 3.1, the resulting beam will have the following polarization vector:

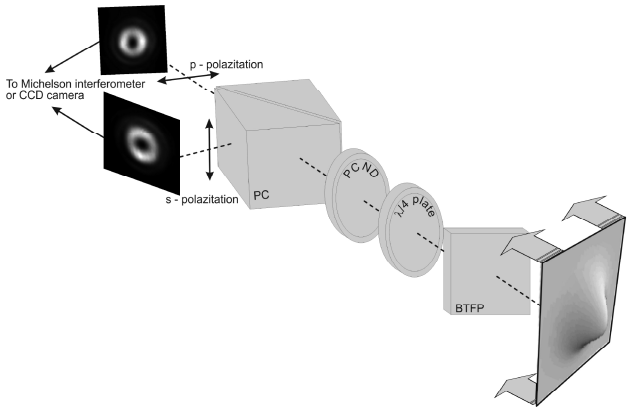

Figure 3.1: The experimental setup (Stage 1 : the unit-charged vortex). BTFP - Brewster thin-film polarizer, PCND -the radial polarization converter, PC - polarization beam splitter.

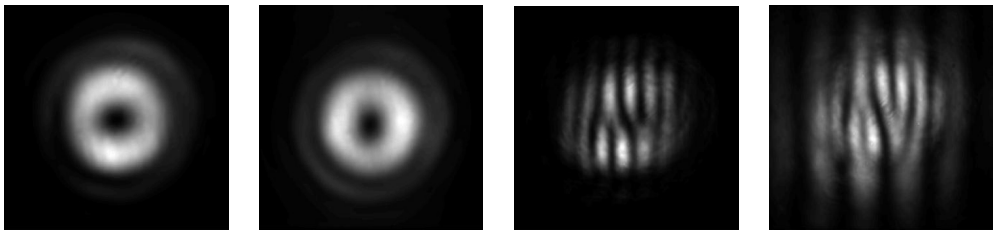

(a) (b) (c) (d)

Figure 3.2: The experimental results : the s (a) and p (b) polarization components and their interference patterns ((c) ir (d)) obtained by using the Michelson interferometer.

$$\vec{w} = \sqrt{2}\mathrm{e}^{\mathrm{i}\frac{\phi}{2}} \begin{bmatrix} \sin\left(\frac{\phi}{2} + \frac{\pi}{4}\right) \\ \sin\left(\frac{\phi}{2} - \frac{\pi}{4}\right) \end{bmatrix} \tag{3.5}$$

We can see the azimuthal phase factor $\mathrm{e}^{\frac{\mathrm{i}\phi}{2}}$. In two orthogonal polarization components, there will be two half-charged vortices, oriented by 180 degree angle with respect to each other.

The Experiment

The experiment was carried out in two stages : 1) The Gaussian beam ($\lambda = 532$ nm) was converted into a unit-charged optical vortex. The experimental setup is shown in fig. 3.1. A circularly polarized light beam was formed by using a polarizer (BTFP) and a $\lambda/4$ waveplate. Then, by passing the radial polarization element (the S-waveplate) a unit-charged optical vortex was formed. The intensity distribution and the interference pattern of the beam was captured by using a CCD camera. The results are shown in fig. 3.2. In both polarization components a unit-charged optical vortex can be seen (as indicated by the fork in interference patterns).

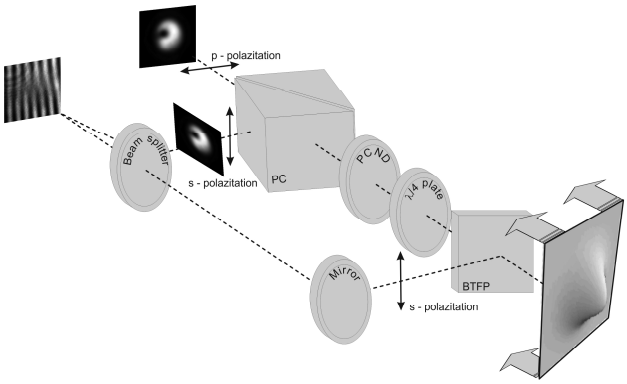

Figure 3.3: The experimental setup (Stage 2 : the half-charged vortex). BTFP - the brewster thin-film polarizer PCND - the radial polarization converter, PC - the polarization beam splitter.

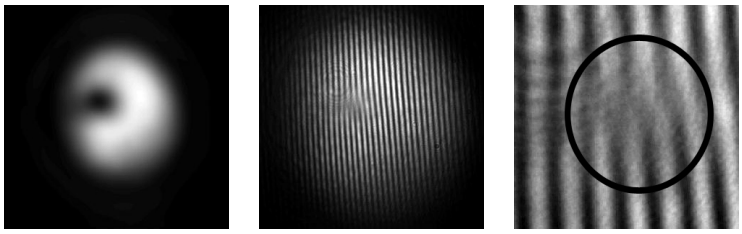

(a) (b) (c)

Figure 3.4: The experimental results : The intensity pattern of one of the vortices' polarization components (a), the interference pattern with a Gaussian beam in the near field (b) and the magnified central part of the interference pattern (c)

2) The experimental setup (as shown in fig. 3.3) was assembled and a half-charged optical vortex was generated. The wavelength of light used in this part of the experiment was $\lambda = 1064$ nm. The generated vortex was superimposed with a Gaussian beam and the resulting interference pattern was captured using a CCD camera. The results are shown in fig. 3.4. In fig. 3.4 (c) a phase shift of $= pi$ between the interference fringes is visible.

Conclusions

It has been shown both theoretically and experimentally that by using a radial polarization converter it is possible to form a unit-charged as well as half-charged optical vortices. In order to obtain a half-charged vortex, it is necessary to use a light beam that has double wavelength than the radial polarization element was designed for.

4. Formation of doubly charged optical vortices by radial polarization converter by using a double-pass technique

It is well known that a radial polarization converter can be used to create unit-charge optical vortices [61]. In this chapter we present a new method which can be used to form the doubly-charged optical vortices by using only a single radial polarization converter. The results of this work have been published in the article [P4] and presented in the conference [K2]

Effect of radial polarization converter on optical vortices

The Jones matrix of a radial polarization converter is :

$$\widehat{J}_{SW} = \begin{bmatrix} \cos\phi & \sin\phi \\ \sin\phi & -\cos\phi \end{bmatrix} . \tag{4.1}$$

The radial polarization converter can change the topological charge of the incoming circularly polarized optical vortex by one. Supposing the input beam is :

$$\vec{v}(\rho,\phi) = A_l(\rho) \begin{bmatrix} 1 \\ \pm\mathrm{i} \end{bmatrix} e^{\mathrm{i}l\phi} , \tag{4.2}$$

where $A_l(\rho)$ is the beam's envelope. It can be shown that the output beam will have the following polarization vector :

$$\vec{w}(\rho,\phi) = A_l(\rho) \begin{bmatrix} 1 \\ \mp i \end{bmatrix} e^{i(l\mp 1)\phi} . \tag{4.3}$$

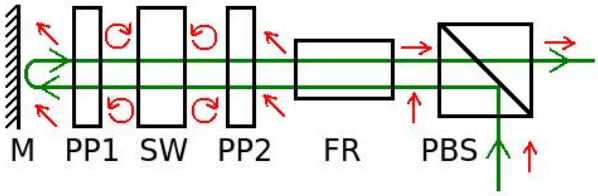

Figure 4.1: The conceptual double-pass setup. M- mirror, PBS - polarization beam splitter, FR - Faraday's rotator, PP1,PP2 - $\lambda/4$ waveplates, SW - the radial polarization converter (the S-waveplate). The arrows show the polarization states of the beam in respective positions.

We see that the topological charge is changed by 1 and the direction of circular polarization is inverted.

Introducing the polarization's handedness coefficient $p = \pm 1$, which shows the direction of the circular polarization (+1 - clockwise, -1 - counter-clockwise), the absolute value of the topological charge can be written : written :

$$|m| = \begin{Bmatrix} |l| + 1, \ l \cdot p > 0 \\ |l| - 1, \ l \cdot p < 0 \end{Bmatrix} . \tag{4.4}$$

Eq. (4.4) shows the conditions when the topological charge increases or decreases. If the winding direction of the helical wavefront coincides with the direction of circular polarization then the absolute value of the topological charge increases, otherwise - decreases.

The principle of the double-pass technique

The conceptual double-pass setup is shown in fig. 4.1. A linearly polarized beam is reflected from a polarization beam splitter (PBS) and passes through a Faraday's rotator FR. Then it passes through a $\lambda/4$ waveplate and becomes circularly polarized. The radial polarization converter SW transforms a circularly polarized Gaussian beam into an unit-charged optical vortex. Further, the beam passes through a $\lambda/4$ waveplate PP1, is reflected from the mirror and again passes through PP1, thus the direction of polarization is inverted. This way, it is ensured that a beam passing back through the radial polarization element SW has proper polarization, so that the topological charge increases. Then the beam passes through the $\lambda/4$ waveplate PP2, then through the Faraday's rotator FR and exits through PBS.

It is important to note that the Faraday's rotator and the polarization beam splitter are not essential in this setup. Instead, a simple beam splitter could be used,

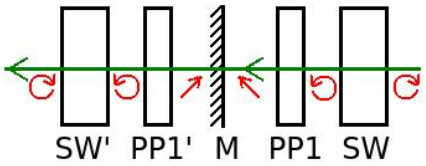

Figure 4.2: The imaginary setup : PP1 - $\lambda/4$ waveplate, SW - the radial polarization element (the S-waveplate), M - mirror, SW' and PP1' - the "reflected" optical components.

however, in this case the efficiency would be reduced, which, even in the ideal case, would be at most 25 percent.

For calculation purposes, it is possible to re-imagine a part of the experimental setup as shown in fig. 4.2. The SW' and PP1' are the "mirrored" optical components, which are reflections of the SW and PP1. The Jones matrix of such system can be written :

$$\widehat{Q} = \widehat{J}_{SW'}\widehat{J}_{SW} = \begin{bmatrix} \cos 2\phi & \sin 2\phi \\ -\sin 2\phi & \cos 2\phi \end{bmatrix} . \tag{4.5}$$

A circularly polarized beam with a polarization vector $\vec{v}$:

$$\vec{v} = \frac{1}{\sqrt{2}} \begin{bmatrix} 1 \\ \mathrm{i} \end{bmatrix} \tag{4.6}$$

will transform into a doubly-charged optical vortex :

$$\vec{w} = \widehat{Q}\vec{v} = \frac{\mathrm{e}^{2\mathrm{i}\phi}}{\sqrt{2}} \begin{bmatrix} 1 \\ i \end{bmatrix} , \tag{4.7}$$

where $\widehat{Q}$ is the Jones matrix from the eq. (4.5). We see, that in eq. (4.7) there is a phase factor $\mathrm{e}^{2\mathrm{i}\phi}$, which is characteristic of an optical vortex with topological charge $l = 2$. The polarization of this beam is circular, but as it passes through the waveplate PP2 (fig. 4.1), it becomes linear.

Of course, converters for higher order optical vortices can also be created. In general, if the waveplate is created to form an optical vortex of topological charge l, then its Jones matrix will be :

$$\widehat{J}_{SW} = \begin{bmatrix} \cos l\phi & \sin l\phi \\ \sin l\phi & -\cos l\phi \end{bmatrix} . \tag{4.8}$$

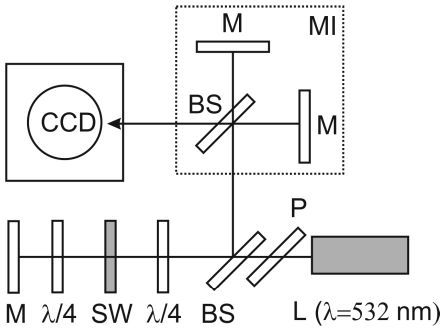

Figure 4.3: The experimental setup. L - the light source, P - poliarizer, BS - beam splitters, $\lambda/4$ - $\lambda/4$ waveplates, M - mirrors, SW - theradial polarization converter, MI - the Michelson interferometer, CCD - a CCD camera.

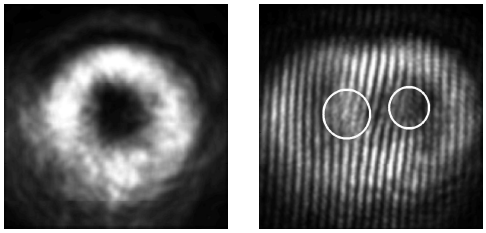

(a) (b)

Figure 4.4: The experimental results : the intensity pattern of the optical vortex (a) and the interference pattern after the Michelson interferometer (b). The fork in the interference pattern indicates the presence of an optical vortex with topological charge $l = 2$.

Following the same calculations as before, it can be shown that the double-pass setup will have a Jones matrix :

$$\widehat{Q} = \begin{bmatrix} \cos 2l\phi & \sin 2l\phi \\ -\sin 2l\phi & \cos 2l\phi \end{bmatrix} . \tag{4.9}$$

It is easy to prove that such experimental setup would create an optical vortex with topological charge $|2l|$.

The Experiment

The experimental setup is shown in fig. 4.3. The light source emits a light beam of $\lambda = 532$ nm. The light is polarized by a polarizer P. After passing through the beam splitter BS, the beam goes through the system $\lambda/4$-SW-$\lambda/4$-M and comes back. The beam, reflected from the beam splitter BS is recorder using the CCD camera. Additionally, using the Michelson interferometer, an interference pattern can be registered proving that there is an optical vortex with topological charge $l = 2$ (fig. 4.4). The fork in the interference pattern clearly indicate the presence of an optical vortex

with second topological charge.

Conclusions

A new technique was proposed, allowing to create a doubly-charged optical vortex by using a single radial polarization converter. This technique has been analyzed theoretically and demonstrated experimentally. Interferometric measurements confirm the presence of a double-charged optical vortex at the output of the experimental setup.

5. Control of optical vortex positions by interference

In this chapter we overview a method allowing to control optical vortex positions by interference. The results of this work have been published in the article [P1] and presented in the conference [K4].

Collinear interference of the Laguerre-Gaussian beams

The collinear interference of two Laguerre-Gaussian beams was analyzed in [7, 8]. In this section it will be only briefly reviewed. Let us consider the following situation : we have two collinear Laguerre-Gaussian modes with topological charges m and l and the radial index equal to zero. Their amplitudes can be written :

$$E_1(\rho,\phi,z) = \mathrm{A}_{01}\frac{\mathrm{W}_{01}}{W_1(z)}\left(\frac{\rho}{W_1(z)}\right)^{|m|}\mathrm{e}^{-\frac{\rho^2}{W_1^2(z)}}\mathrm{e}^{\mathrm{i}\left(\mathrm{k}z+m\phi+\mathrm{k}\frac{\rho^2}{2R_1(z)}-\eta_1(z)\right)}\ , \tag{5.1a}$$

$$E_2(\rho,\phi,z) = \mathrm{A}_{02}\frac{\mathrm{W}_{02}}{W_2(z)}\left(\frac{\rho}{W_2(z)}\right)^{|l|}\mathrm{e}^{-\frac{\rho^2}{W_2^2(z)}}\mathrm{e}^{\mathrm{i}\left(\mathrm{k}z+l\phi+\mathrm{k}\frac{\rho^2}{2R_2(z)}-\eta_2(z)+\Phi_0\right)}\ . \tag{5.1b}$$

In eqs. 5.1a and 5.1b, W_{01} and W_{02} are the beam's waist radii, $W_1(z)$ and $W_2(z)$ are the beam radii at z, $R_1(z)$ and $R_2(z)$ are the wavefront curvature radii, $\eta_1(z)$ and $\eta_2(z)$ are the Gouy phases. $\Phi_0$is the phase difference between the beams. For Laguerre-Gaussian beams, these parameters can be expressed as follows :

$$W(z) = \mathrm{W}_0\sqrt{1+(z/\mathrm{l}_d)^2}\ , \tag{5.2a}$$

$$R(z) = z\left(1+(\mathrm{l}_d/z)^2\right)\ , \tag{5.2b}$$

$$\eta(z) = (|m|+1)\arctan\left(z/\mathrm{l}_d\right)\ , \tag{5.2c}$$

$$\mathrm{l}_d = \mathrm{k}\mathrm{W}_0^2/2\ . \tag{5.2d}$$

In eq. 5.2d l_d is the diffraction length, also known as the "Rayleigh length". It

shows at what distance from the waist the beam radius increases $\sqrt{2}$ times.

The positions of optical vortices will be found from the following equation :

$$E = E_1 + E_2 = 0 \ . \tag{5.3}$$

The coordinates of the optical vortices can be obtained at $z = const$:

$$\rho = W(z) \left(\frac{A_2}{A_1} \right)^{\frac{1}{|m|-|l|}} \ , \tag{5.4a}$$

$$\phi = \frac{(2n+1)\pi + \Phi_0}{m-l} \ , \tag{5.4b}$$

where n is an integer ($0 \leq n < |m-l|$ for each dislocation at $\rho = 0$), and the amplitudes A_1 and A_2 in the eq. (5.4a) are :

$$A_1 = \mathrm{A}_{01}\mathrm{W}_0/W(z) \ , \tag{5.5a}$$

$$A_2 = A_{02}W_0/W(z) \ . \tag{5.5b}$$

Also, if $l \neq 0$, there will be a dislocation in the center of the beam which has a topological charge $m - l$.

Eqs. (5.4a) and (5.4b) show that the position of the optical vortex depends only on the ratio of the amplitudes and the angular position depends only on the phase difference between the beam. Thus, it is possible to control the optical vortex positions in two transverse coordinates independently. However, this is only true if the wavefront curvature radii of the beams are the same. Otherwise, the angular position of the vortices will also depend on the ratio of the beams' amplitudes.

Eq. (5.4a) can be rewritten to include the maximum intensities of the beams :

$$\rho = \frac{W(z)}{\sqrt{2\mathrm{e}}} \sqrt{\frac{\mathrm{I}_{2max}|m|^{|m|}}{\mathrm{I}_{1max}|l|^{|l|}}}^{\frac{1}{|m|+|l|}} \ . \tag{5.6}$$

The results of numerical modeling are shown in fig. (5.1) (see the next page). It is possible to see that by changing the intensity ratio we can control the radial position of the vortex. Also, by changing the phase difference the whole beam can be rotated around its axis.

Also it should be mentioned that if the beam radii are not the same, it is possible for secondary dislocations to appear and annihilate.

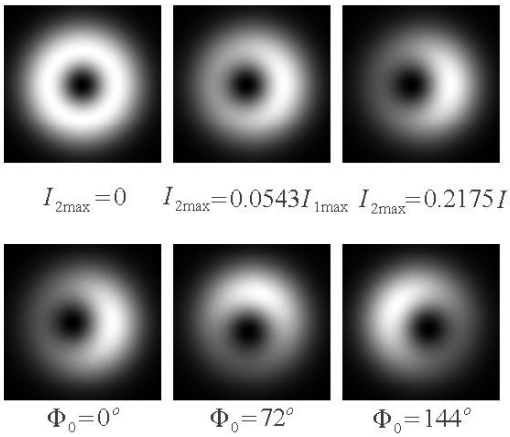

Figure 5.1: Numerical results : the intensity pattern of the combined beam from an unit-charged optical vortex (I_1) and a Gaussian beam (I_2). In the top row : different intensity ratios, in the bottom row : different phase differences.

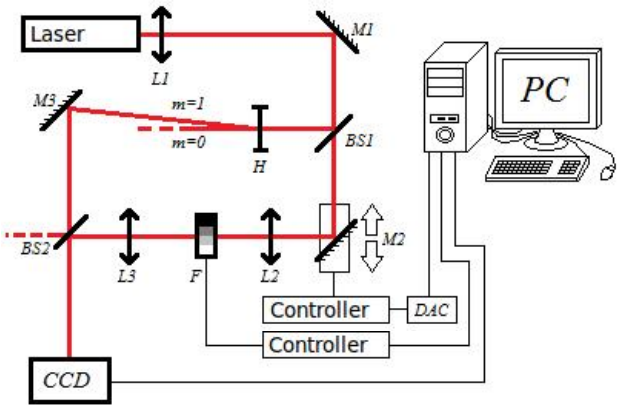

Figure 5.2: The experimental setup : M1-M3 - mirrors, L1-L3 - lens, BS1-BS2 - beam splitters, F - variable transparency filter, H - an optical vortex hologram, DAC - digital-analog converter, PC - a computer.

The Experiment

A computerized vortex controller was implemented experimentally. The experimental setup is shown in fig. 5.2. A HeNe laser ($\lambda = 632.8$ nm) was chosen for the experiment. The beam was split into two parts, one part was used as a reference beam and from the other part an optical vortex was generated. Then these two beams were joined in a collinear way. The phase difference was controlled by the mirror M2, which was mounted on a piezoelectric translation stage and the intensity ration was controlled by a variable transparency filter F. The phase and intensity of the reference beam was controlled from computer.

The experimental results are shown in fig. (5.3). It is possible to see that the vortices can be rotated by changing the phase difference and can be translated in the radial direction by changing the intensity ratio of the beams. Also, optical vortices

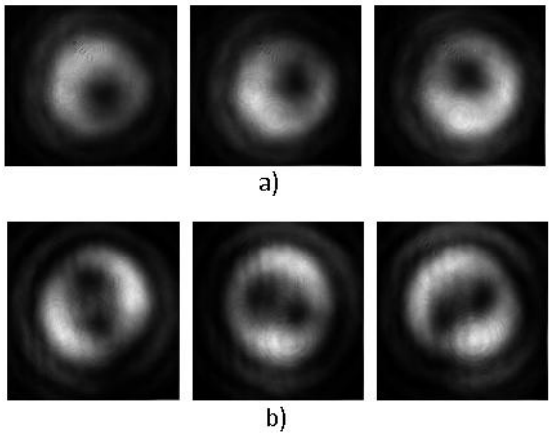

Figure 5.3: Intensity patterns of the combined beam from an optical vortex and a Gaussian beam (experimental results) : a) topological charge $m = 1$, b) $m = 2$. Phase differences (from left to right) : $\Delta\Phi = 0^o$, $\Delta\Phi = 90^o$, $\Delta\Phi = 180^o$.

with topological charge $|m| > 1$ are unstable and decay to a set of unit-charged vortices.

Conclusions

It was shown theoretically and experimentally that is it possible to control optical vortex positions by collinear interference between an optical vortex and a Gaussian beam. Formulas have been derived allowing to calculate optical vortex positions based on the intensity ratio and the phase difference of the superimposing beams. The advantage of this method is that it is not limited by the optical damage threshold. However, the it is only possible to control unit-charged vortices, since the higher-order vortices decay in presence of a coherent background. Also, the maximum range of optical vortex motion is limited.

6. Conservation of topological charge in a second harmonic generation process for fractional-charge optical vortices

In this chapter we investigate the topological charge conservation for fractional charge optical vortices. The results of this work have been published in the article [P5] and presented in the conference [K3].

The dilemma of topological charge conservation of fractional-charge optical vortices

Let us take simple example of the second harmonic generation. The pump depletion and walk-off can be neglected. Then, the equation for the second harmonic beam looks like this:

$$2\mathrm{ik}_2\frac{\partial A_2}{\partial z}+\frac{1}{\rho}\frac{\partial}{\partial\rho}\left(\rho\frac{\partial A_2}{\partial\rho}\right)+\frac{1}{\rho^2}\frac{\partial A_2}{\partial\phi}=\mathrm{i}\sigma_2 A_1^2(\rho,\phi,z)\mathrm{e}^{\mathrm{i}\Delta\mathrm{k}z} \tag{6.1}$$

where $A_2(\rho,\phi,z)$ is the complex amplitude of the second harmonic, $A_1(\rho,\phi,z)$ is the complex amplitude of the first harmonic and Δk is the phase mismatch. if the fist harmonic is an optical vortex with topological charge l, t. y. $A_1(\rho,\phi,z)\propto\exp(\mathrm{i}l\phi)$, then the equation (6.1) will have a solution with double azimuthal phase modulation: $A_2(\rho,\phi,z)\propto\exp(\mathrm{i}2l\phi)$.

This topological charge conservation should be valid for any vortices : with integer or fractional topological charge . However, the fractional-charge vortices are unstable and decay into optical vortices with the nearest topological charge [5, 6]. Then the question arises, which topological charges will add up in the nonlinear process : the integer or the fractional? This question will be addressed in further sections.

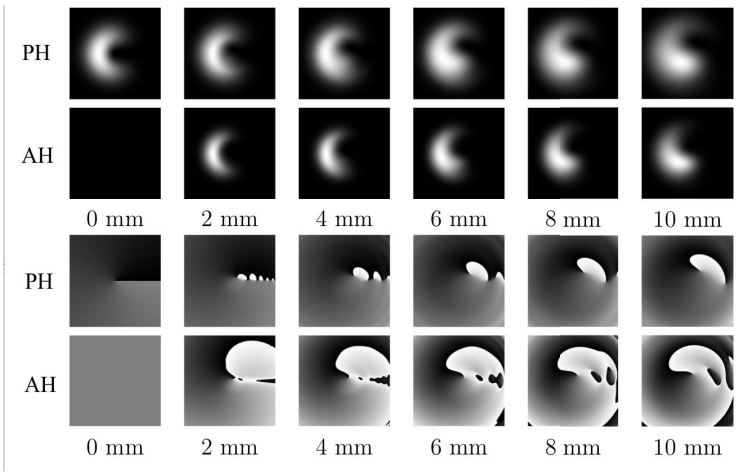

Figure 6.1: Results of the numerical simulation : the first harmonic (PH) and the second harmonic (AH) intensity patterns (top) and phase maps (bottom). In the second harmonic, approximately in the center of the beam a unit-charged vortex is visible.

Topological charge conservation in the second harmonic generation process

Numerical modeling and the experimental results show, the second harmonic generated by a half-charged vortex, will carry a unit-charge vortex. To explain this phenomenon, the following equations have been simulated numerically :

$$2\mathrm{ik}_1\frac{\partial A_1}{\partial z} + \nabla_T^2 A_1 = \mathrm{i}\sigma_1 A_2^* A_1 \exp(-\mathrm{i}\Delta\mathrm{k}z) \tag{6.2a}$$

$$2\mathrm{ik}_2\frac{\partial A_2}{\partial z} + \nabla_T^2 A_2 = \mathrm{i}\sigma_2 A_1^2 \exp(\mathrm{i}\Delta\mathrm{k}z) \tag{6.2b}$$

The full phase matching has been assumed ($\Delta k = 0$), the walk-off was also neglected. The refractive indices have been chosen for both waves $\mathrm{n}_1 = \mathrm{n}_2 = 1.5$ without attachment to any particular crystal. The length of the nonlinear crystal was in the simulation was 10 mm. The results of numerical simulations are shown in fig. 6.1.

In fig. 6.1 we can see that approximately in the center of the second harmonic beam, a unit-charged optical vortex is present, despite the fact that the fractional-charged vortex transforms into a unit-charged vortex. It happens due to the fact that the transformation of the first harmonic beam into a unit-charged optical vortex happens in the dark area of the beam which does not contribute much into the second harmonic generation. The phase of the second harmonic beam is influenced by the bright part of the first harmonic beam.

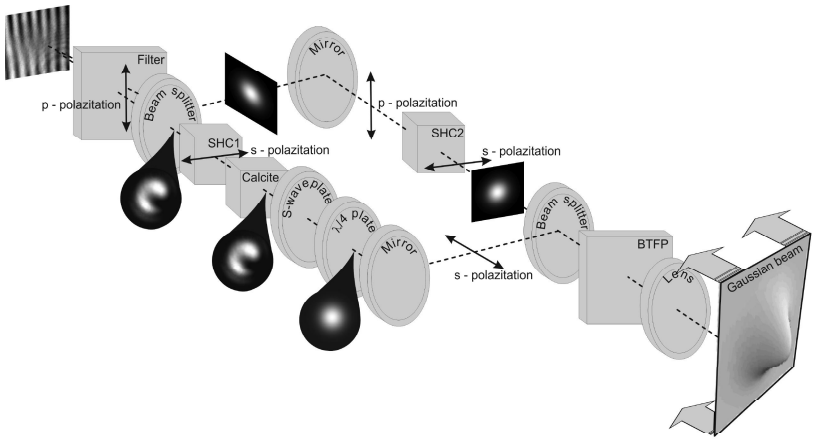

Figure 6.2: The experimental setup. SHC1,SHC2 - the nonlinear crystals and BFTP - brewster thin-film polarizer.

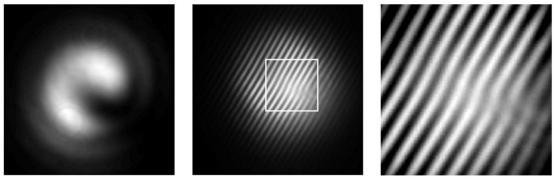

Figure 6.3: The experimental results : the first harmonic beam. (a) - the intensity pattern, (b) - the interference pattern, (c) - the magnified central part of the interference pattern. The phase shift og π is visible between the interference fringes.

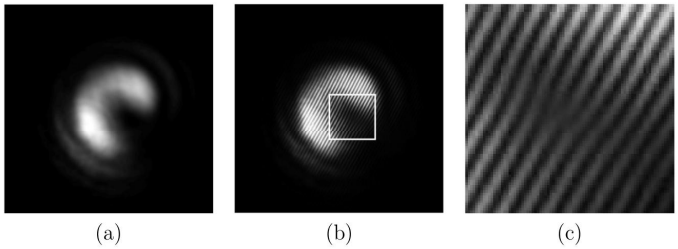

Figure 6.4: The experimental result : the second harmonic beam. (a) - the intensity pattern, (b) - the interference pattern, (c) - the magnified central part of the interference pattern. In the center of the interference pattern, a fork is visible, which is characteristic of unit-charged optical vortex.

The Experiment

In order to determine the topological charges of the optical vortices, a Mach-Zehnder interferometer was used. The experimental setup is shown in fig. 6.2. A STA-01CW laser was used as the light source (wavelength $\lambda = 1064$ nm). A Gaussian beam was collimated, as shown in the schematic, by lens and then divided by a beam

splitter into two branches : one of them was for the reference beam and the other one for the optical vortex. The reference beam is meant only for the interferometric measurements. It produceas a second-harmonic Gaussian beam in the crystal SHC2. At the output, the reference and the vortex beams are brought together again by the use of a beam splitter. After filtering off the remains of the first harmonic, a second-harmonic beam was registered using a CCD camera (or, if the reference beam is not blocked, then the interference pattern ir registered). By changing the filter, the remains of the first harmonic were registered as well. The results are shown in figs. 6.3 and 6.4.

The first harmonic beam has the phase characteristic of a half-charged optical vortex (fig. 6.3), while in the center of the second harmonic interference pattern, a fork is visible (fig. 6.4 (c)), which proves the existence of a unit-charged optical vortex in the second harmonic beam. Therefore, we have experimental proof of topological charge conservation for half-charged optical vortices.

Conclusions

It has been shown both theoretically and experimentally that the topological charge conservation law is valid for a half-charged optical vortex in the second harmonic generation process despite the decay of the vortex. This happens because the second harmonic is generated in the bright part of the beam and its phase characteristic influences the second harmonic beam the most, while the decay happens in the dark part of the beam and does not influence second harmonic.

7. Generation of beams with polarization singularities using the optical parametric amplification of optical vortices

In this chapter, a new way to form beams with polarization singularities is presented.

Generation of beams with polarization singularities by superposition of Laguerre-Gaussian modes

Beams with polarization singularities can be formed by superposition of two Laguerre-Gaussian modes [74, 75, 76]. A detailed analysis has been given in works [74, 75]. In here, we define only two classes of beams which are significant for our purposes :

$$\begin{aligned} \vec{v}_l^{(1)} = A(r) \begin{bmatrix} \cos l\phi \\ \sin l\phi \end{bmatrix} = \\ = \tfrac{1}{2} A(r) \left(\exp(\mathrm{i}l\phi) \begin{bmatrix} 1 \\ -\mathrm{i} \end{bmatrix} + \exp(-\mathrm{i}l\phi) \begin{bmatrix} 1 \\ \mathrm{i} \end{bmatrix} \right) \end{aligned} \tag{7.1}$$

and

$$\begin{aligned} \vec{v}_l^{(2)} = A(r) \begin{bmatrix} -\sin l\phi \\ \cos l\phi \end{bmatrix} = \\ = \tfrac{\mathrm{i}}{2} A(r) \left(\exp(\mathrm{i}l\phi) \begin{bmatrix} 1 \\ -\mathrm{i} \end{bmatrix} - \exp(-\mathrm{i}l\phi) \begin{bmatrix} 1 \\ \mathrm{i} \end{bmatrix} \right) \end{aligned} . \tag{7.2}$$

which we will call as the radial-type (eq. (7.1)) and azimuthal-type (7.2)) since in

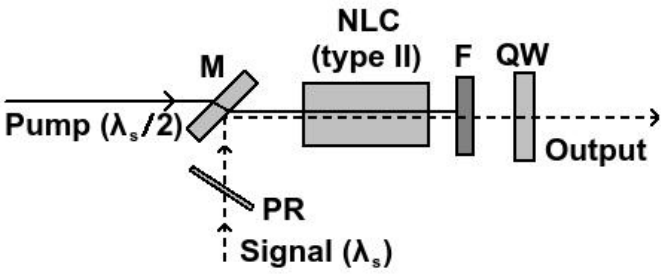

Figure 7.1: The conceptual experimental setup : M - a mirror, PR - a phase regulator (a thin glass plate which can be rotated to change the optical path of the beam), NLC - a type-II nonlinear crystal, F - filter, which absorbs the pump beam and QW -a quater-waveplate. The pump beam is Gaussian and the signal is an optical vortex. At the output the beam has a polarization singularity

the simplest case of $l = 1$, they have radial and azimuthal polarization respectively. The l is the topological charge of the optical vortices and $A(r)$ is the envelope of the beam which depend only on the radial coordinate. We can see that radial and azimuthal type beams with polarization singularities can be expressed as a superposition of two oppositely-charged optical vortices wit opposite handedness circular polarization.

The general idea of the method

The main idea is to obtain a beam with polarization singularity from two oppositely charged optical vortices. Such optical vortices can be obtained in optical parametric amplification process since a topological charge conservation law holds true.

The conceptual experimental setup is shown in fig. 7.1. The signal and pump beams are joined by using the wavelength-selective mirror M and are amplified in the nonlinear crystal NLC. The NLC has a type-II phase matching so that the polarizations of the outgoing signal and idler waves are perpendicular and the interaction is degenerate with respect to the wavelength. The phase regulator PR selects the proper phase of the signal beam. It is actually a glass plate which, when rotated, changes the optical path of the signal beam. At the output, the quarter-waveplate QW transforms the combined signal-idler beam into a beam with a polarization singularity. The quarter-waveplate has to be properly oriented at an angle of 45 degrees. The Jones matrix of a properly the rotated waveplate should be :

$$\widehat{A} = \begin{bmatrix} 1 & -\mathrm{i} \\ -\mathrm{i} & 1 \end{bmatrix} . \tag{7.3}$$

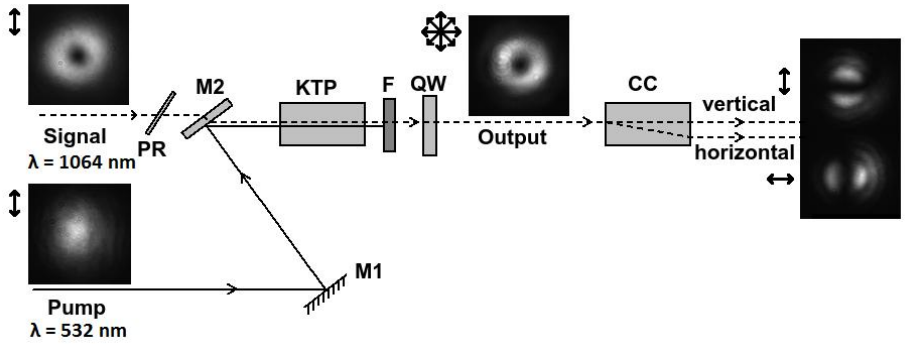

Figure 7.2: The experimental setup along with the results. PR -the phase regulator, M1 - a mirror, M2 - wavelength-selective mirror, KTP - the nonlinear crystal, QW - the quarter-waveplate, CC - the calcite crystal.

Let us discuss two cases:

1) When there is $\pi/2$ phase difference between the signal and idler wave. Then, after the crystal we have the output polarization vector:

$$\vec{v} = \begin{bmatrix} \exp(\mathrm{i}l\phi) \\ \mathrm{i}\exp(-\mathrm{i}l\phi) \end{bmatrix} . \tag{7.4}$$

As it passes through the quarter-waveplate, it will transform in the following way :

$$\vec{w} = \begin{bmatrix} 1 & -\mathrm{i} \\ -\mathrm{i} & 1 \end{bmatrix} \begin{bmatrix} \exp(\mathrm{i}l\phi) \\ \mathrm{i}\exp(-\mathrm{i}l\phi) \end{bmatrix} = 2 \begin{bmatrix} \cos(l\phi) \\ \sin(l\phi) \end{bmatrix} . \tag{7.5}$$

At the output, we will have a radial-type beam.

2) Another case, when the phase difference between the signal and idler wave is $-\pi/2$. Then ,after the quarter-waveplate we obtain an azimuthal-type beam:

$$\vec{w} = \begin{bmatrix} 1 & -\mathrm{i} \\ -\mathrm{i} & 1 \end{bmatrix} \begin{bmatrix} \mathrm{i}\exp(\mathrm{i}l\phi) \\ \exp(-\mathrm{i}l\phi) \end{bmatrix} = 2 \begin{bmatrix} -\sin(l\phi) \\ \cos(l\phi) \end{bmatrix} . \tag{7.6}$$

Yet another type of beams will be obtained if the quarter-waveplate is rotated to the opposite direction.

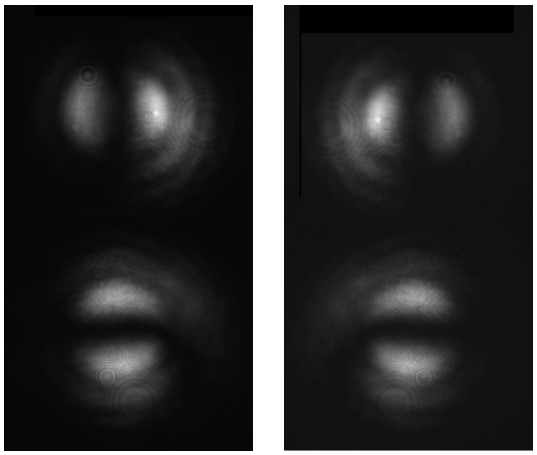

(a) (b)

Figure 7.3: Vertical (top) and horizontal (bottom) polarization components of the outgoing radial (a) and azimuthal (b) polarization beams.

Experimental

The experimental idea has already been discussed. The experimental setup was assembled as shown in fig. 7.2. The polarization structure of the resulting beams has been confirmed by analysis using a birefringent calcite crystal. The radial and azimuthal beams have been produced using this method. Both radially and azimuthally polarized beams have been obtained as can be seen from the split polarization components in fig. 7.3.

Conclusions

A new method has been experimentally demonstrated and theoretically analyzed, which allows to generate radially and azimuthally polarized beams. This can also produce higher order polarization singularities.

8. The main results and conclusions

1. It has been shown both theoretically and experimentally that by using a radial polarization converter it is possible to obtain a unit-charged or a half-charged optical vortex by using a circularly polarized Gaussian beam. In order to create a half-charged vortex, a light beam of double wavelength (compared to the wavelength for which the radial polarization element was designed for)is needed.

2. A new technique to create a doubly-charged optical vortex with an S-waveplate was created and investigated both theoretically and experimentally. It has bees shown that by using a double-pass technique, a doubly-charged optical vortex can be obtained.

3. It has been shown both theoretically and experimentally that is it possible to control optical vortices' positions by a collinear interference with a Gaussian beam. This method is not limited by the optical damage threshold. However, multiply-charged optical vortices decay into unit-charged vortices. Also, the maximum amplitude of the vortex motion is limited.

4. It has been theoretically and experimentally confirmed that for the half-charged vortex, despite it inherent instability, the topological charge conservation holds true in the second harmonic generation process. This happens because the second harmonic beam is mainly influenced by the bright part of the first harmonic beam and the decay of the half-charged vortex happens in the dark part, which does not contribute much to the second harmonic generation.

5. A new method to create beams with polarization singularities was created and demonstrated experimentally. Radially and azimuthally polarized beams have been created by using this method.

Bibliography

[1] J. F. Nye, M. V. Berry. Dislocations in wave trains. P. Roy. Soc. Lond. A: Mat., **336**(1605), 165–190 (1974)

[2] P. Coullet, L. Gil, F. Rocca. Optical vortices. Opt. Commun., **73**, 403–408 (1989)

[3] M. Dienerowitz, M. Mazilu, P. J. Reece, T. F. Krauss, K. Dholakia. Optical vortex trap for resonant confinement of metal nanoparticles. Opt. Express, **16**(7), 4991–4999 (2008)

[4] S. W. Hell, J. Wichmann. Breaking the diffraction resolution limit by stimulated emission: stimulated-emission-depletion fluorescence microscopy. Opt. Lett., **19**(11), 780–782 (1994)

[5] T. Ali, L. Kreminska, A. B. Golovin, D. T. Crouse. Propagation of optical vortices with fractional topological charge in free space (2014)

[6] I. V. Basistiy, M. S. Soskin, M. V. Vasnetsov. Optical wavefront dislocations and their properties. Opt. Commun., **119**, 604–612 (1995)

[7] M. S. Soskin, V. N. Gorshkov, M. V. Vasnetsov, J. T. Malos, N. R. Heckenberg. Topological charge and angular momentum of light beams carrying optical vortices. Phys. Rev. A, **56**, 4064–4075 (1997)

[8] P. Stanislovaitis, V. Smilgevičius. Control of optical vortex dislocations using optical methods. Lit. J. Phys., **52**(4), 295–300 (2012)

[9] F. A. Bovino, M. Braccini, M. Giardina, C. Sibilia. Orbital angular momentum in noncollinear second-harmonic generation by off-axis vortex beams. J. Opt. Soc. Am. B, **28**(11), 2806–2811 (2011)

[10] A. Bekshaev, M. Soskin, M. Vasnetsov. Paraxial Light Beams with Angular Momentum. ArXiv e-prints (2008)

[11] L. Allen, M. W. Beijersbergen, R. J. C. Spreeuw, J. P. Woerdman. Orbital angular momentum of light and the transformation of laguerre-gaussian laser modes. Phys. Rev. A, **45**, 8185–8189 (1992)

[12] N. B. Simpson, L. Allen, M. J. Padgett. Optical tweezers and optical spanners with laguerre–gaussian modes. J. Mod. Opt., **43**(12), 2485–2491 (1996)

[13] M. V. Vasnetsov, I. G. Marienko, M. S. Soskin. Self-reconstruction of an optical vortex. J. Exp. Theor. Phys. Lett., **71**(4), 130–133 (2000)

[14] A. Chernykh, A. Bekshaev, A. Khoroshun, L. Mikhaylovskaya, A. Akhmerov, K. A. Mohammed. Edge diffraction of optical-vortex beams formed by means of the fork hologram (2015)

[15] I. G. Marienko, M. S. Soskin, M. V. Vasnetsov. Diffraction of optical vortices (1999)

[16] V. N. Gorshkov, A. N. Koroshun, M. S. Soskin. Diffraction of the singular beam on an opaque screen and regeneration of an optical vortex. Ukr. J. Phys., **51**(2) (2005)

[17] A. Bekshaev, L. Mikhaylovskaya, A. Chernykh, A. Khoroshun. Evolution of the phase singularities in edge-diffracted optical-vortex beams. ArXiv e-prints (2016)

[18] J. Durnin, J. J. Miceli, J. H. Eberly. Diffraction-free beams. Phys. Rev. Lett., **58**, 1499–1501 (1987)

[19] W. Lee, X.-C. Yuan, K. Dholakia. Experimental observation of optical vortex evolution in a gaussian beam with an embedded fractional phase step. Opt. Commun., **239**(1–3), 129 – 135 (2004)

[20] M. S. Soskin, M. V. Vasnetsov. Nonlinear singular optics. Pure Appl. Opt. A, **7**(2), 301 (1998)

[21] I. Basistiy, V. Bazhenov, M. Soskin, M. Vasnetsov. Optics of light beams with screw dislocations. Opt. Commun., **103**(5), 422 – 428 (1993)

[22] K. Dholakia, N. B. Simpson, M. J. Padgett, L. Allen. Second-harmonic generation and the orbital angular momentum of light. Phys. Rev. A, **54**, R3742–R3745 (1996)

[23] S.-M. Li, L.-J. Kong, Z.-C. Ren, Y. Li, C. Tu, H.-T. Wang. Managing orbital angular momentum in second-harmonic generation. Phys. Rev. A, **88**, 035801 (2013)

[24] D. V. Petrov, L. Torner. Observation of topological charge pair nucleation in parametric wave mixing. Phys. Rev. E, **58**, 7903–7907 (1998)

[25] D. V. Petrov, G. Molina-Terriza, L. Torner. Vortex evolution in parametric wave mixing. Opt. Commun., **162**(4–6), 357 – 366 (1999)

[26] A. Beržanskis, A. Matijošius, A. Piskarskas, V. Smilgevičius, A. Stabinis. Sum-frequency mixing of optical vortices in nonlinear crystals. Opt. Commun., **150**, 372–380 (1998)

[27] A. Beržanskis, A. Matijošius, A. Piskarskas, V. Smilgevičius, A. Stabinis. Conversion of topological charge of optical vortices in a parametric frequency-converter. Opt. Commun., **140**, 273–276 (1997)

[28] A. Berzanskis, A. Matijosius, A. S. Piskarskas, V. Smilgevicius, A. Stabinis. Parametric amplification of an optical vortex (1997)

[29] V. Pyragaite, A. Piskarskas, K. Regelskis, V. Smilgevicius, A. Stabinis, S. Mikalauskas. Parametric down-conversion of higher-order bessel optical beams in quadratic nonlinear medium. Opt. Commun., **240**(1–3), 191 – 200 (2004)

[30] G. Molina-Terriza, J. P. Torres, L. Torner. Orbital angular momentum of photons in noncollinear parametric downconversion. Opt. Commun., **228**(1–3), 155 – 160 (2003)

[31] J. Arlt, K. Dholakia, L. Allen, M. J. Padgett. Parametric down-conversion for light beams possessing orbital angular momentum. Phys. Rev. A, **59**, 3950–3952 (1999)

[32] Y.-C. Lin, Y. Nabekawa, K. Midorikawa. Conical third-harmonic generation of optical vortex through ultrashort laser filamentation in air. Opt. Express, **24**(13), 14857–14870 (2016)

[33] G. X. Li, S. M. Chen, Y. Cai, S. Zhang, K. W. Cheah. Third harmonic generation of optical vortices using holography-based gold-fork microstructure. Advanced Optical Materials, **2**(4), 389–393 (2014)

[34] P. Hansinger, A. Dreischuh, G. G. Paulus. Optical vortices in self-focusing kerr nonlinear media. Opt. Commun., **282**(16), 3349 – 3355 (2009)

[35] P. Polynkin, C. Ament, J. V. Moloney. Self-focusing of ultraintense femtosecond optical vortices in air. Phys. Rev. Lett., **111**, 023901 (2013)

[36] C.-C. Jeng, M.-F. Shih, K. Motzek, Y. Kivshar. Partially incoherent optical vortices in self-focusing nonlinear media. Phys. Rev. Lett., **92**, 043904 (2004)

[37] J. Christou, V. Tikhonenko, Y. S. Kivshar, B. Luther-Davies. Vortex soliton motion and steering. Opt. Lett., **21**(20), 1649–1651 (1996)

[38] C. P. S. N. R. Heckenberg, R. McDuff, A. G. White. Generation of optical phase singularities by computer-generated holograms. Opt. Lett., **17**(3), 221–223 (1992)

[39] A. V. Carpentier, H. Michinel, J. R. Salgueiro, D. Olivieri. Making optical vortices with computer-generated holograms. Am. J. Phys., **76** (1988)

[40] V. Y. Bazhenov, M. V. Vasnetsov, M. S. Soskin. Laser beams with screw dislocations in their wavefronts. Pis'ma Zh. Eksp. Teor. Fiz., **52**(8), 429–431 (1990)

[41] A. Y. Bekshaev, A. S. Bekshaev, K. Mohammed. Arrays of optical vortices formed by 'fork' holograms. Ukr. J. Phys. Opt., **15**, 123 (2014)

[42] S. Topuzoski. Generation of optical vortices with curved fork-shaped holograms. Opt. Quant. Electron., **48**(2), 138 (2016)

[43] M. Beijersbergen, R. Coerwinkel, M. Kristensen, J. Woerdman. Helical-wavefront laser beams produced with a spiral phaseplate. Opt. Commun., **112**(5–6), 321 – 327 (1994)

[44] C. Jun, K. Deng-Feng, G. Min, F. Zhi-Liang. Generation of optical vortex using a spiral phase plate fabricated in quartz by direct laser writing and inductively coupled plasma etching. Chinese Phys. Lett., **26**(1), 014202 (2009)

[45] J. F. Algorri, V. Urruchi, B. Garcia-Cámara, J. M. Sánchez-Pena. Generation of optical vortices by an ideal liquid crystal spiral phase plate. IEEE Electr. Device L., **35**(8), 856–858 (2014)

[46] V. Kotlyar, A. Kovalev, R. Skidanov, S. Khonina, O. Moiseev, V. Soĭfer. Simple optical vortices formed by a spiral phase plate. J. Opt. Technol., **74**(10), 686–693 (2007)

[47] J. Grover A. Swartzlander. The optical vortex lens. Opt. Photon. News, **17**(11), 39–43 (2006)

[48] J. E. Curtis, B. A. Koss, D. G. Grier. Dynamic holographic optical tweezers. Opt. Commun., **207**(1–6), 169 – 175 (2002)

[49] D. McGloin, G. Spalding, H. Melville, W. Sibbett, K. Dholakia. Applications of spatial light modulators in atom optics. Opt. Express, **11**(2), 158–166 (2003)

[50] R. W. Gerchberg, W. O. Saxton. A practical algorithm for the determination of phase rom image and diffraction plane pictures. Optik, **35**(2), 237–246 (1972)

[51] A. Jesacher, A. Schwaighofer, S. Fürhapter, C. Maurer, S. Bernet, M. Ritsch-Marte. Wavefront correction of spatial light modulators using an optical vortex image. Opt. Express, **15**(9), 5801–5808 (2007)

[52] N. Matsumoto, T. Ando, T. Inoue, Y. Ohtake, N. Fukuchi, T. Hara. Generation of high-quality higher-order laguerre-gaussian beams using liquid-crystal-on-silicon spatial light modulators. J. Opt. Soc. Am. A, **25**(7), 1642–1651 (2008)

[53] Y. Lu, B. Jiang, S. Lü, Y. Liu, S. Li, Z. Cao, X. Qi. Arrays of Gaussian vortex, Bessel and Airy beams by computer-generated hologram. Opt. Commun., **363**, 85–90 (2016)

[54] E. Abramochkin, V. Volostnikov. Beam transformations and nontransformed beams. Opt. Commun., **83**(1), 123 – 135 (1991)

[55] J. Courtial, M. Padgett. Performance of a cylindrical lens mode converter for producing laguerre–gaussian laser modes. Opt. Commun., **159**(1–3), 13 – 18 (1999)

[56] M. J. Padgett, L. Allen. Orbital angular momentum exchange in cylindrical-lens mode converters. J. Opt. B - Quantum S. O., **4**(2), S17 (2002)

[57] M. Beijersbergen, L. Allen, H. van der Veen, J. Woerdman. Astigmatic laser mode converters and transfer of orbital angular momentum. Opt. Commun., **96**(1), 123 – 132 (1993)

[58] T. Hasegawa, T. Shimizu. Frequency-doubled hermite–gaussian beam and the mode conversion to the laguerre–gaussian beam. Opt. Commun., **160**(1–3), 103 – 108 (1999)

[59] A. T. O'Neil, J. Courtial. Mode transformations in terms of the constituent hermite–gaussian or laguerre–gaussian modes and the variable-phase mode converter. Opt. Commun., **181**(1–3), 35 – 45 (2000)

[60] M. Beresna, M. Gecevicius, P. G. Kazansky. Polarization sensitive elements fabricated by femtosecond laser nanostructuring of glass. Opt. Mater. Express., **1**(4) (2011)

[61] M. Beresna, M. Gecevicius, P. G. Kazansky, T. Gertus. Radially polarized optical vortex converter created by femtosecond laser nanostructuring of glass. Appl. Phys. Lett., **98**(201101) (2011)

[62] Y. Shimotsuma, P. G. Kazansky, J. Qiu, K. Hirao. Self-organized nanogratings in glass irradiated by ultrashort light pulses. Phys. Rev. Lett., **91**(24) (2003)

[63] A. Forbes. Controlling light's helicity at the source: orbital angular momentum states from lasers. Philos. Tr. R. Soc. S - A, **375**(2087) (2017)

[64] R. Oron, N. Davidson, A. A. Friesem, E. Hasman. Efficient formation of pure helical laser beams. Opt. Commun., **182**(1–3), 205 – 208 (2000)

[65] A. Ito, Y. Kozawa, S. Sato. Generation of hollow scalar and vector beams using a spot-defect mirror. J. Opt. Soc. Am. A, **27**(9), 2072–2077 (2010)

[66] D. Naidoo, K. Aït-Ameur, M. Brunel, A. Forbes. Intra-cavity generation of superpositions of laguerre–gaussian beams. Appl. Phys. B, **106**(3), 683–690 (2012)

[67] I. A. Litvin, L. Burger, A. Forbes. Petal-like modes in porro prism resonators. Opt. Express, **15**(21), 14065–14077 (2007)

[68] M. P. Thirugnanasambandam, Y. Senatsky, K. Ueda. Generation of very-high order laguerre-gaussian modes in yb:yag ceramic laser. Laser Phys. Lett., **7**(9), 637 (2010)

[69] K. Kano, Y. Kozawa, S. Sato. Generation of a purely single transverse mode vortex beam from a he-ne laser cavity with a spot-defect mirror. International Journal of Optics, **2012**(359141) (2012)

[70] M. Beresna, M. Gecevičius, N. M. Bulgakova, P. G. Kazansky. Twisting light with micro-spheres produced by ultrashort light pulses. Opt. Express, **19**(20), 18989–18996 (2011)

[71] R. K. Tyson, M. Scipioni, J. Viegas. Generation of an optical vortex with a segmented deformable mirror. Appl. Opt., **47**(33), 6300–6306 (2008)

[72] D. P. Ghai, P. Senthilkumaran, R. S. Sirohi. Adaptive helical mirror for generation of optical phase singularity. Appl. Opt., **47**(10), 1378–1383 (2008)

[73] D. P. Ghai. Generation of optical vortices with an adaptive helical mirror. Appl. Opt., **50**(10), 1374–1381 (2011)

[74] S. Vyas, Y. Kozawa, S. Sato. Polarization singularities in superposition of vector beams. Opt. Express, **21**(7), 8972–8986 (2013)

[75] S. Vyas, Y. Kozawa, Y. Miyamoto. Creation of polarization gradients from superposition of counter propagating vector lg beams. Opt. Express, **23**(26), 33970–33979 (2015)

[76] C.-H. Yang, Y.-D. Chen, S.-T. Wu, A. Y.-G. Fuh. Independent manipulation of topological charges and polarization patterns of optical vortices. Scientific reports, **6** (2016)